Design of Filters With Reduced Fabrication Tolerance for 5G Application

Francis Emmanuel Chinda
Department of Computer Engineering
Federal University Wukari
Taraba State, Nigeria
francischinda@fuwukari.edu.ng

Socheatra Soeung
Dept. of Elect/Electronic Engineering
Universiti Teknologi Petronas
Sri Iskandar,Perak, Malaysia
socheatra.s@utp.edu.my

Cheab Sovuthy
School of Digital Engineering
Cambodia Academy of Dig. Technology
Phnom Penh, Cambodia
sovuthy.cheab@cadt.edu.kh

James Okpor
Department of Computer Engineering
Federal University Wukari
Taraba State, Nigeria
okporjames@fuwukari.edu.ng

Huzein Fahmi Hawari
Dept.Elect/ Electronic Engineering
Universiti Teknologi Petronas
Sri Iskandar,Perak, Malaysia
huzeinfahmi.hawari@utp.edu.my

Surajo Alh.Musa
Dept. of Elect /Electronic Engineering
The Federal University of Tech.Babura
Jigawa State, Nigeria
samusa.ele@futb.edu.ng

***Abstract*—This paper presents a novel design of compact filters with reduced fabrication tolerance for 5G applications. The filter will offer a reduced sensitivity to fabrication processes and maintain its response matched to traditional Chebyshev filters. The transfer function is derived using chained filtering functions (CFFs) for fourth-order filters. The design technique is demonstrated using circuit simulation carried out in advanced simulation software (ADS) and high-frequency simulation software (HFSS). The prototype of the filter is fabricated using parallel-connected open-loop microstrip resonators. The overall compact size is 2.5cm x 4cm. The simulation and measured insertion/return loss are 0.40dB / 20dB and 2.6dB/18 dB. Sensitivity analysis is conducted to confirm its enhanced tolerance to fabrication variations, validating the theoretical analysis. The prototype filter is validated and agrees with the theoretical investigation. The results show significant improvements in filter performance, including reduced insertion loss, enhanced selectivity, and increased stability across varying operating conditions. This work provides valuable insights and practical solutions for engineers and researchers aiming to optimize 5G network infrastructure with high-precision, compact filters.**

Keywords—compact filters, fabrication processes, 5G applications, selectivity, Stability

I. INTRODUCTION

Filter design Engineers are under constant pressure to realize filters with reduced tuning time and cost for front-end subsystem applications [1]. Designing a compact filter with high performance requires superior materials, a precise fabrication machine, and, post-production tuning. Efforts in electromagnetic (EM) simulation tools have been made to enhance the design of such filters [2]. These challenges have been shifted to manufacturing processes due to improved simulation tools. To completely appreciate the advantages of simulation precision, the hardware must be designed and manufactured with a very low tolerance level [3].

Currently, most of the filters that are being designed and produced are made from the Chebyshev class [6]. With a specified filter order, this class gives the best attenuation response [4]. The frequency distribution in the Chebyshev filter passband is a critical element in getting a good response [5]. The frequency separation at higher order becomes very small, requiring a very precise fabrication process [6]. A tuning is applied after fabrication to return the filter response to the desired response for implementation. To solve this problem, sensitivity to the fabrication processes and the limitations of current fabrication technologies must be taken into account at the design preliminary stage and approximation [7]. This can be achieved by simulating the filter specifications using a higher-order transfer function. Low-order seed functions of Chebyshev polynomials can be multiplied to form a new class of filtering function called Chained [8]. The filtering function is a trade-off between Butter-worth and Chebyshev approximations, it bridges the benefits of both Butter-worth and Chebyshev functions [9]. The technique will provide several transfer functions to choose from, each with distinct features and realization specifications. The transfer functions will have the ability to reduce filter design complexity, fabrication sensitivity, and tuning processes [10]. This can extend the state-of-the-art to realize higher-order filters with better performance and can be implemented at high frequencies.

This paper introduces the design of a novel filter with reduced fabrication tolerance for 5G applications. Fourth-order filter prototype will be fabricated using an open-loop microstrip structure. Considerable sensitivity analysis is conducted to prove the fabrication tolerance of the filter.

II. THE FILTERING FUNCTION

A. Seed Filtering Function Formation

The filtering function can be formed by multiplying the Chebyshev polynomial of the first kind [11], [12]. The seed function is generated using maple-soft software following the outlined procedure. Table 1 shows the combinations of seed functions for a fourth-order filter N = 4.

TABLE I. THE SEED FUNCTION COMBINATION FOR N = 4

No. of Seed Function	Seed-Function Order	Polynomial Function
4	{1,1,1,1}	ω^4
3	{1,1,2}	$2\omega^4 - \omega^2$
2	{2,2}	$4\omega^4 - 4\omega^2 + 1$
2	{3,1}	$4\omega^4 - 3\omega^2$
1	{4}	$8\omega^4 - 8\omega^2 + 1$

The first and last rows in the table are Butterworth and Chebyshev polynomials. The polynomials rows in between the chained function polynomials.

III. CIRCUIT SIMULATION

The circuit simulation is carried out using advanced simulation software (ADS). The network is formed using the J-admittance values derived in (1). The extracted low-pass values of the filter network are shown in Tab II and the circuit S-parameter response is in Fig. 2.

TABLE II. THE LOW-PASS VALUES OF THE FILTER NETWORK

Components	Low-Pass Values
$C_1 = C_2$	1.09F
$C_3 = C_4$	2.16F
$J_{S1} = J_{2L}$	1
$J_{S3} = J_{4L}$	1
J_{12}	0.83
J_{34}	-3.3023

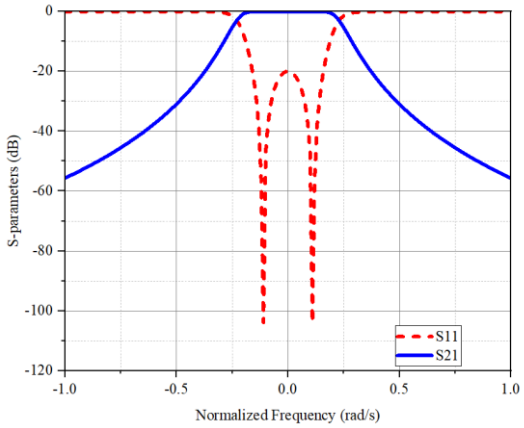

Figure 2: The Low-Pass S-Parameter Response

The values of the low-pass prototype can be modified into a band-pass filter using the suitable transformation equations in [13]. The modified values of inductance and capacitances are summarized in Tab III and the bandpass S-parameter response is in Fig. 3.

TABLE III. THE BANDPASS VALUES OF THE FILTER NETWORK

Parameters	Band-Pass Values
$L_1 = L_2$	0.002nH
$L_3 = L_4$	1.015nH
$C_1 = C_2$	991.4pF
$C_3 = C_4$	748.4pF
J_{12}	0.828
J_{34}	-3.302

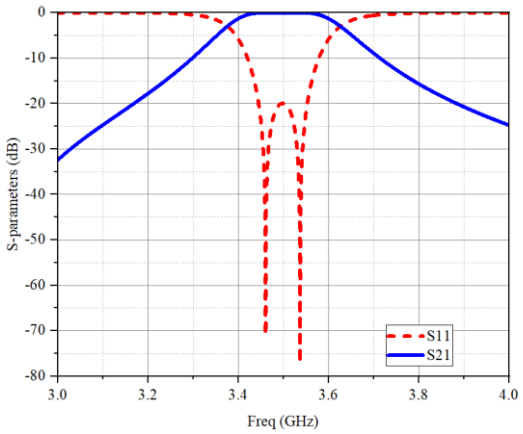

Figure 3: The Bandpass S-Parameter Response

This process is useful in synthesizing different parallel layout circuits such as four and six-branch networks.

A. *The Filter Coupling Matrix*

The filter coupling matrix is derived by using the appropriate equations in [14]. The matrix is mapped by multiplying the seed functions generated from {2,2} polynomial. The S-parameters S_{11} and S_{21} are used to derive the filter coupling matrix using the equations in [15], and [16]. A reduction method can also be used to derive the coupling matrix structure through which the rows of the matrix can be achieved [17]. Similarity transformation is carried out on the matrix of sub-network to get the coupling combinations. The overall coupling matrix, M, includes coupling from source to load is presented in [18]

IV. THE FILTER REALIZATION

The filter simulation is conducted using microstrip (open loop) resonators [19]. These resonators are chosen due to ease of tuning and their inherent characteristics of reducing sensitivity. The length (L) and Width (W) of the resonators are derived using the microstrip synthesis method. In Tab.VI presents the initial specifications of the design.

TABLE IV. THE DESIGN SPECIFICATIONS

Parameters	**Specifications**
Center Frequency	3.5GHz
Bandwidth	≥ 40 MHz
Filter Order	4
Insertion Loss	≤ 3 dB

Substrate	RT/Roger Duroid 5880
Substrate Thickness	787 µm
Copper Clad-Thickness	17.5 µm
Relative Dielectric Constant (εr)	2.2
Loss tangent (tanδ)	0.009
Electrical Length	180°
Resonator Length (L)	3.15mm
Resonator Width (W)	2.45mm

A. *The Filter Resonator Coupling*

The Inter-resonator coupling can be achieved by carefully adjusting the gap or distance between the resonators. The adjacent resonators coupling is a mixed configuration [20]. The coupling coefficient (K) values are determined using the line calculation technique in advanced design software (ADS).

The strength of the coupling (K) increases as the distance (S) decreases and vice versa. This implies that weaker coupling is associated with smaller coefficient values, while stronger coupling is associated with larger coefficient values. A 0.5mm gap is specified in this design to enhance resonator coupling. The filter input and output terminals are configured as source (S) and load (L). The source is connected to the resonator's input, while the load is to the output.

B. *The Filter Layout Design*

The synthesized values in [10] are transformed into a physical network to realize the fourth-order filter. The layout design is performed using advanced design software (ADS). The resonator's topologies are connected in parallel and chained to the output. Fig.5 shows the filter's physical layout while Fig.6. presents its S-parameters response.

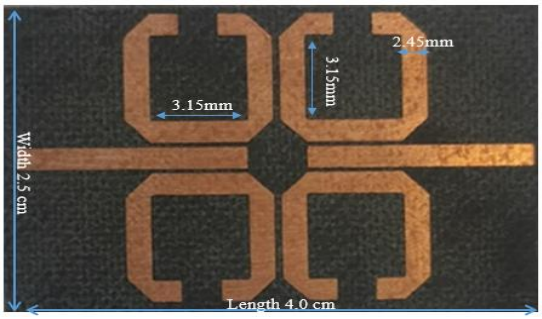

Figure 5: The Filter Physical Layout

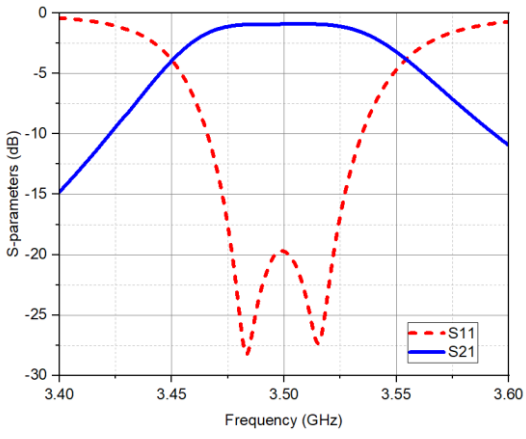

Figure 6: The Filter Layout S-Parameter Response

The layout has generated 2-poles as expected at the center frequency of 3.5GHz. This result demonstrates the main advantage of the polynomials which place multiple return-loss at the same frequency resulting in producing filters that are less sensitive to fabrication tolerance and still maintaining their performance compared to the Chebyshev counterpart. Compared to the theoretical analysis, the filters have proven to provide good rejection. This ability depends on the choice of optimal seed function.

V. THE PROTOTYPE DESIGN AND RESULTS

The filter prototype is fabricated on an RT/Roger Duroid 5880 substrate, with a thickness of 787 µm and a copper cladding of 17.5 µm. The substrate dielectric constant (εr) is 2.2 and a loss tangent (tan δ) of 0.0009 [12]. The microstrip electrical length is 180° which is half a wavelength [21]. The dimensions of the resonators are 2.45 mm (width) and 3.15 mm (length). SMA connectors of 3.5 mm are connected to the input and output ports of the filter. The feed lines of 10mm are used to link the resonators to the connectors. Fig.7 shows the fabricated filter prototype while Fig.8 presents the measured S-parameter performance.

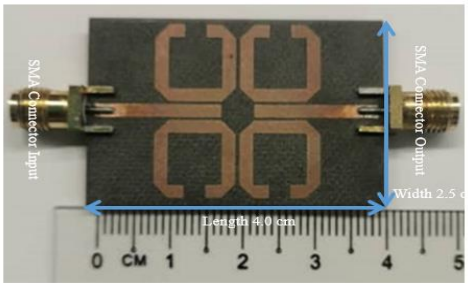

Figure 7: The Filter Prototype

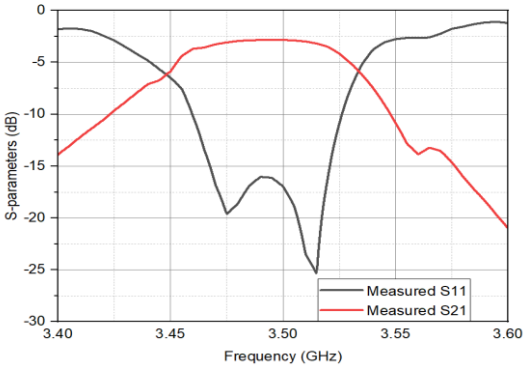

Figure 8: The Prototype Measured S-Parameter Response

The filter-measured result is summarized in Tab. VI.

TABLE V. THE FILTER MEASURED RESULTS

Parameters	Results
The overall size	2.5cm × 4cm
The center frequency	3.49 GHz
The measured insertion loss (IL)	2.83 dB
The measured return loss (RL)	16.2 dB
Achieved bandwidth (BW)	50.4 MHz

Fractional bandwidth	1.44%
The out of -band rejection	20.7 dB
Selectivity	89.68

The prototype has met the requirements to produce 2-poles at the center frequency of 3.5GHz as expected. This outcome has proven that the filter is compact with good performance in terms of insertion loss, return loss, and selectivity.

A. *Comparison of Simulation and Measured Results*

The filter simulation/measured insertion and return loss are 00.89dB/20dB and 2.9dB/16 dB. The simulated/measured bandwidths are 46.8 MHz/ 50.4 MHz, and the simulated/measured fractional bandwidths (FBW) are 1.3% /1.4%. Fig.9 shows the simulated and measured S-parameter response.

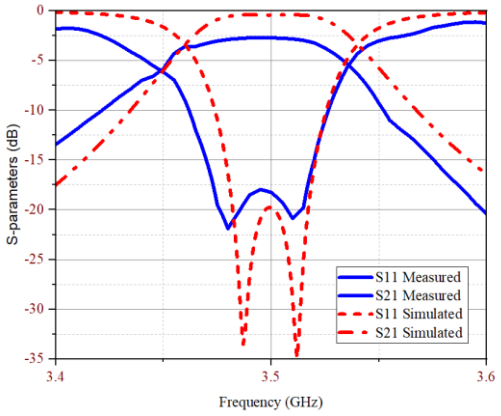

Figure 9: The Filter Simulated and Measured S-Parameter Response

These results confirm that the filter is efficient with good performance in terms of selectivity. A small shift of 0.1% is observed in the measured bandwidth and 1% in insertion loss. The shift may be due to factors such as electrical discontinuities, calibration cable loss, SMA soldering port, ground effects, and improper handling of fabrication processes. Also, the shift in insertion loss may be due to mesh setup (mesh refinement, mesh density) and environmental factors such as temperature, humidity, electromagnetic interference, or improper handling of fabrication processes such as fabrication setup, equipment aging, SMA connector soldering ground effects and calibration cable loss. This filter is suitable for applications where high-performance filtering is required such as 5G and satellite systems. The slight variation in the measured bandwidth should be taken into consideration for specific practical applications.

B. *The Filter Sensitivity Analysis*

Sensitivity analysis is conducted to prove the filter prototype fabricated tolerance compared to Chebyshev counterpart i.e. to validate how the filter responds to changes with variations in its component's values. The analysis helps in identifying parameters or variables that are most critical to the filter performance and can guide the designer to optimize its performance and mitigate potential challenges. The analysis is conducted on the values of the low-pass component in ADS to validate the impact of tolerance on the filter. In this work, a tolerance of ± 0.5% and ± 1%, are selected and applied. The maximum tolerance is selected based on the provided approximation of fabrication machines. Tabs VII, VIII, and IX summarize the variables, and Fig.10. and 10 display the filter S-parameter response (performance) when tolerance is applied.

TABLE VI. VARIATIONS OF APPLIED ±0.5% TOLERANCE

Parameters	Original value	Tol. of +0.5%	Tol. of -0.5%
C_1	1.09	1.07	1.09
C_2	1.08	1.07	1.09
C_3	2.16	2.1	2.14
C_4	2.16	2.1	2.14

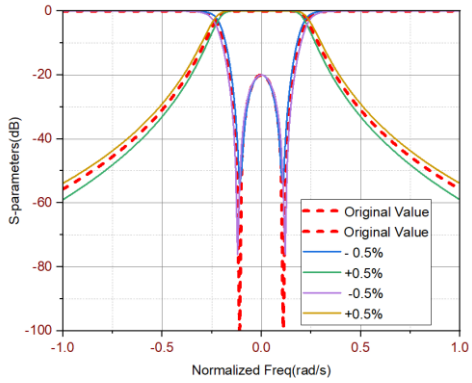

Figure 10: The Impacts of Applied ± 0.5% Tolerance on the Filter

TABLE VII. VARIATIONS OF APPLIED ±2% TOLERANCE

Parameters	Original value	Tol. of +1%	Tol. of -1%
C_1	1.08	1.06	1.10
C_2	1.08	1.06	1.10
C_3	2.16	2.12	2.18
C_4	2.16	2.12	2.18

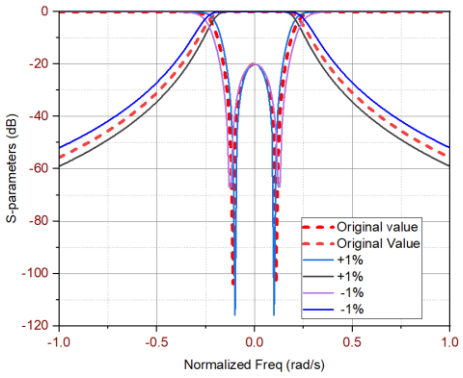

Figure 11: The Impacts of Applied ± 1% Tolerance on the Filter

These findings greatly prove the reliability of the filter in terms of sensitivity to fabrication errors and selectivity when random tolerance is applied. The further apart placement of poles is achieved and confirms higher fabrication tolerance.

VI. CONCLUSION

A new filter with reduced sensitivity to manufacturing tolerance was introduced and fabricated. The size of the filter is 2.5cm x 4cm. Design and simulation were conducted using advanced simulation software (ADS). The simulated and measured insertion/ return loss are 0.40 dB / 20dB and 2.6 dB/18 dB. The measured results were analyzed and validated and in good agreement with the theory. A considerable sensitivity analysis was conducted to prove its fabrication tolerance and reliability are comparable to the Chebyshev counterpart. The filter is compact and suitable for application at 5G and satellite systems. The realization of this filter is not limited to only microstrip technology and topology but to any available technology. Lower- and higher-order filters can easily be realized using this technique, thereby serving as a very valuable tool for any design engineer.

ACKNOWLEDGMENT

The authors thank the Federal University of Wukari and the Tertiary Education Trust Fund (TETFUND) for funding this research. The authors appreciate everyone who contributed, directly or indirectly, to completing this project.

.

REFERENCES

[1] S. Li, S. Li, J. Yuan, J. Liu, and M. Shi, "Fully Tunable Bandpass Filter with Wide Bandwidth Tuning Range and Switchable Single/Dual Band," *IEEE Access*, vol. 12, pp. 36577–36585, 2024.

[2] L. Wu, Y. Wu, Y. Yao, R. Huang, Z. Xu, and W. Wang, "Dual-Band Bandpass Filter with Controllable Transmission Zeros Using Multimode GGW Cavity," *IEEE Microwave and Wireless Technology Letters*, 2024

.

[3] Z. Zhang *et al.*, "Microwave Displacement Sensors Based on Filtering Phase Shifter with Chebyshev Response," *IEEE Sens J*, vol. 24, no. 10, pp. 15857–15864, May 2024.

[4] M. Wang, G. Liu, Y. Wu, J. Zhou, and Z. Cheng, "Reconfigurable Bandpass Filter with Multi-Band Switching and Band Shiftability," *IEEE Transactions on Circuits and Systems II: Express Briefs*, Jun. 2024.

[5] Z. Zhang *et al.*, "Microwave Displacement Sensors Based on Filtering Phase Shifter with Chebyshev Response," *IEEE Sens J*, vol. 24, no. 10, pp. 15857–15864, May 2024.

[6] D. C. H. Bong, V. Jeoti, S. Cheab, and P. W. Wong, "Design and Synthesis of Chained-Response Multiband Filters," *IEEE Access*, vol. 7, pp. 130922–130936, 2019.

[7] Y. P. Lim, Y. L. Toh, S. Cheab, G. S. Ng, and P. W. Wong, "Chained-Function Waveguide Filter for 5G and beyond," *IEEE Region 10 Annual International Conference, Proceedings/TENCON*, vol. 2018-Octob, no. October, pp. 107–110, 2019.

[8] Y. P. Lim, S. Cheab, S. Soeung, and P. W. Wong, "On the design and fabrication of chained-function waveguide filters with reduced fabrication sensitivity using CNC and DMLS," *Progress In Electromagnetics Research B*, vol. 87, no. January, pp. 39–60, 2020.

[9] L. Zhu, R. Payapulli, S. H. Shin, M. Stanley, N. M. Ridler, and S. Lucyszyn, "3-D Printing Quantization Predistortion Applied to Sub-THz Chained-Function Filters," *IEEE Access*, vol. 10, pp. 38944–38963, 2022.

[10] F. E. Chinda, S. Cheab, and S. Soeung, "Design and Synthesis of Parallel-Connected Dielectric Filter Using Chain-Function Polynomial," vol. 32, no. 1, pp. 51–62, 2023.

[11] P. W. Wong, "A Sustainable and Fast Approach to Filter Design for 5G Implementation," *RFM 2018 - 2018 IEEE International RF and Microwave Conference, Proceedings*, vol. 88, no. 3, pp. 349–351, 2018.

[12] S. Cheab, P. W. Wong, and S. Soeung, "Design of multi-band filters using parallel connected topology," *Radioengineering*, vol. 27, no. 1, pp. 186–192, 2018.

[13] T. Huang, H. Liu, C. Guo, L. Feng, and L. Geng, "3-D Printed mm-Wave Filter Using Increased-Height DGS Resonator for Spurious Suppression," *IEEE Transactions on Circuits and Systems II: Express Briefs*, vol. 69, no. 11, pp. 4293–4297, 2022.

[14] V. B. Narayane and G. Kumar, "A Selective Wideband Bandpass Filter with Wide Stopband Using Mixed Lumped-Distributed Circuits," *IEEE Transactions on Circuits and Systems II: Express Briefs*, vol. 69, no. 9, pp. 3764–3768, 2022.

[15] T. K. Das, S. Chatterjee, S. K. A. Rahim, and T. K. Geok, "Compact High-Selectivity Wide Stopband Microstrip Cross-Coupled Bandpass Filter with Spurline," *IEEE Access*, vol. 10, no. July, pp. 69866–69882, 2022.

[16] K. Zhao and D. Psychogiou, "Single-to-Multi-Band Reconfigurable Acoustic-Wave-Lumped-Resonator Bandpass Filters," *IEEE Transactions on Circuits and Systems II: Express Briefs*, vol. 69, no. 4, pp. 2066–2070, 2022.

[17] G. Lin, S. Member, Y. Dong, and S. Member, "A Compact, Hybrid SIW Filter With Controllable Transmission Zeros and High Selectivity," vol. 69, no. 4, pp. 2051–2055, 2022.

[18] F. E. Chinda, S. Seoung, M. S. Yahya, S. Cheab, and H. F. Hawari, "Design of High-Performance Parallel-Connected Filters Using Chained Filtering Functions," 2023.

[19] H. S. Im and S. W. Yun, "Design of a dual-band bandpass filter using an open-loop resonator," *Journal of Electromagnetic Engineering and Science*, vol. 17, no. 4, pp. 197–201, 2017.

[20] Z. Xu, Y. Wu, Q. Dong, and W. Wang, "Miniaturized Dual-Band Filter Using Dual-Mode Dielectric Waveguide Resonator," *IEEE Microwave and Wireless Components Letters*, vol. 32, no. 12, pp. 1411–1414, 2022.

[21] Y. Leong, S. Cheab, S. Soeung, and P. W. Wong, "A New Class of Dual-Band Waveguide Filters Based on Chebyshev Polynomials of the Second Kind," *IEEE Access*, vol. 8, pp. 28571–28583, 2020.